This article was downloaded by: [Institute Of Atmospheric Physics]
On: 09 December 2014, At: 15:33
Publisher: Taylor & Francis
Informa Ltd Registered in England and Wales Registered Number: 1072954 Registered office: Mortimer House, 37-41 Mortimer Street, London W1T 3JH, UK

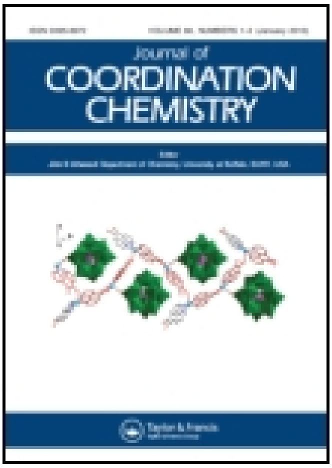

[Click for updates](#)

Journal of Coordination Chemistry
Publication details, including instructions for authors and subscription information:
http://www.tandfonline.com/loi/gcoo20

Diverse structures, weak interactions, and catalytic properties of three palladium 2-sulfobenzoate complexes with 1,10-phenanthroline

Xiao-Li Tang[a], Ai-Qing Ma[ab], Guo-Qiang Cai[ab] & Long-Guan Zhu[a]
[a] Department of Chemistry, Zhejiang University, Hangzhou, PR China
[b] School of Pharmacy, Guangdong Medical College, Dongguan, PR China

Published online: 20 Jan 2014.

To cite this article: Xiao-Li Tang, Ai-Qing Ma, Guo-Qiang Cai & Long-Guan Zhu (2014) Diverse structures, weak interactions, and catalytic properties of three palladium 2-sulfobenzoate complexes with 1,10-phenanthroline, Journal of Coordination Chemistry, 67:3, 449-460, DOI: 10.1080/00958972.2013.867032

To link to this article: http://dx.doi.org/10.1080/00958972.2013.867032

PLEASE SCROLL DOWN FOR ARTICLE

Taylor & Francis makes every effort to ensure the accuracy of all the information (the "Content") contained in the publications on our platform. However, Taylor & Francis, our agents, and our licensors make no representations or warranties whatsoever as to the accuracy, completeness, or suitability for any purpose of the Content. Any opinions and views expressed in this publication are the opinions and views of the authors, and are not the views of or endorsed by Taylor & Francis. The accuracy of the Content should not be relied upon and should be independently verified with primary sources of information. Taylor and Francis shall not be liable for any losses, actions, claims, proceedings, demands, costs, expenses, damages, and other liabilities whatsoever or howsoever caused arising directly or indirectly in connection with, in relation to or arising out of the use of the Content.

This article may be used for research, teaching, and private study purposes. Any substantial or systematic reproduction, redistribution, reselling, loan, sub-licensing, systematic supply, or distribution in any form to anyone is expressly forbidden. Terms &

Journal of Coordination Chemistry, 2014
Vol. 67, No. 3, 449–460, http://dx.doi.org/10.1080/00958972.2013.867032

Diverse structures, weak interactions, and catalytic properties of three palladium 2-sulfobenzoate complexes with 1,10-phenanthroline

XIAO-LI TANG†, AI-QING MA†‡, GUO-QIANG CAI†‡ and LONG-GUAN ZHU*†

†Department of Chemistry, Zhejiang University, Hangzhou, PR China
‡School of Pharmacy, Guangdong Medical College, Dongguan, PR China

(*Received 10 September 2013; accepted 14 November 2013*)

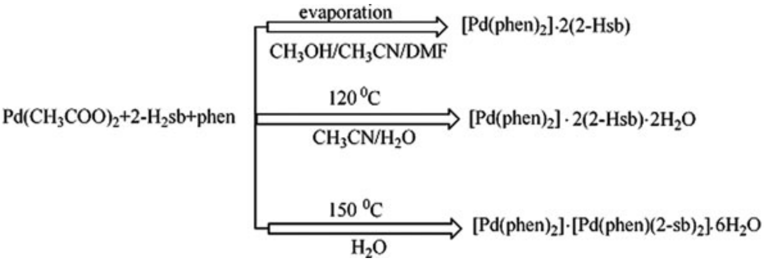

Three complexes with same components, Pd^{II}, 2-sulfobenzoate and 1,10-phenanthroline, $[Pd(phen)_2]\cdot 2(2\text{-}Hsb)$ (**1**), $[Pd(phen)_2](2\text{-}Hsb)\cdot(2\text{-}Hsb)\cdot 2H_2O$ (**2**), and $[Pd(phen)_2]\cdot[Pd(phen)(2\text{-}sb)_2]\cdot 6H_2O$ (**3**), where $2\text{-}H_2sb$ is 2-sulfobenzoic acid and phen is 1,10-phenanthroline, were synthesized and characterized by IR spectra, elemental analyses, thermogravimetric analyses, UV–vis absorption spectra and powder X-ray analysis. Single X-ray crystal structural analyses showed that **1** and **2** are ionic species, while **3** is a dimer through weak bonding interactions. In **1** and **2**, $2\text{-}Hsb^-$ ligands are partly deprotonated and it is fully deprotonated in **3**. In **2** and **3** there are hydrogen bonds and π–π interactions. Extended hydrogen bonding structures for **2** and **3** are 1-D and 3-D architectures, respectively. The oxidation of methyl phenyl sulfide by **1-3** as homogeneous catalysts gave high conversion and selectivity in methanol. The addition of 2-sulfobenzoic acid in the catalytic reaction further promotes the conversion.

Keywords: Palladium complex; 2-Sulfobenzoate; Diverse structure; Catalytic activity

1. Introduction

Sulfobenzoate ligands have one carboxyl and one sulfonate, which can provide coordination sites and hydrogen bonding acceptors or donors [1, 2]. Sulfobenzoate metal complexes have been extensively studied due to interesting topological and functional properties [3–6]. The Pd complexes have been widely used as catalysts in organometallic reactions [7], such as C–C coupling, C–H functionalization, and hydrocarbon oxidation [8–10]. Pd(II) is a soft

---

*Corresponding author. Email: chezlg@zju.edu.cn

Lewis acid and can form strong bonds with nitrogen or sulfur donors [11]. There is no report on Pd complex with sulfobenzoate ligands [12]. Much attention has been focused on weak interactions such as hydrogen bonding, metal–metal, metal…H, π–π stacking, C–H…π and metal…π interactions for Pd(II) complexes, which can play important roles in the properties [13–15], but such investigation is limited. The design and synthesis of complexes in supramolecular chemistry and crystal engineering are attractive because their functional properties are strongly related to their structures. In order to obtain diverse structures for the Pd(II) sulfobenzoate system, the typical N-donor chelate ligand 1,10-phenanthroline (phen) has been chosen for potential aromatic stacking interactions. Construction of coordination compounds is influenced by many factors, such as metal ions, organic ligands, counteranions, experimental temperature, solvent molecules, and pH of the reaction mixture. Herein we report the syntheses, structures, weak interactions, and catalytic properties of three palladium complexes with the same components, $[Pd(phen)_2]\cdot 2(2\text{-}Hsb)$ (**1**), $[Pd(phen)_2](2\text{-}Hsb)\cdot(2\text{-}Hsb)\cdot 2H_2O$ (**2**), and $[Pd(phen)_2]\cdot[Pd(phen)(2\text{-}sb)_2]\cdot 6H_2O$ (**3**), where $2\text{-}H_2sb$ is 2-sulfobenzoic acid and phen is 1,10-phenanthroline.

2. Experimental

2.1. *Materials and instruments*

The chemicals for synthesis were purchased from Aladdin Industrial Corporation and used without purification. Elemental analyses for C, H, and N were performed using a Perkin–Elmer analyzer model 1110. Infrared spectra were obtained on a Nicolet Nexus 470 infrared spectrophotometer as KBr pellets from 400 to 4000 cm^{-1}. Thermal analysis curves (TG) were obtained from a Delta Series TA-SDT Q600 in a nitrogen atmosphere with a heating rate of 10 °C/min using Al_2O_3 crucibles. UV–vis spectra were measured on a SPECORD 2000 UV–vis spectrophotometer in CH_3OH at room temperature. ^1H and ^{13}C NMR spectra were recorded on a Bruker NMR AVANCE^{III} 400 spectrometer. The powder X-ray diffractions were measured by Rigaku D/MaX 2550PC with Cu-Kα radiation. The GC data were recorded on a Fuli Gas Chromatograph equipped with a DB-5 capillary column. All the standards used in GC were purchased from Alfa Aesar.

2.2. *Synthesis*

2.2.1. Preparation of $[Pd(phen)_2]\cdot 2(2\text{-}Hsb)$ (1). A methanol solution (5 mL) of palladium (II) acetate (0.015 g, 0.0668 mM) and 2-sulfobenzoic acid (0.059 g, 0.267 mM) was added to an acetonitrile solution (5 mL) of 1,10-phenanthroline (0.026 g, 0.131 mM). After 10 min stirring at room temperature, 5 mL of DMF (N,N-dimethylformamide) was added to the reaction mixture and stirring was continued for a further 10 min. Then the solution was set aside for slow evaporation. After one day, yellow crystals were obtained and collected by filtration. Yield: 79.6%. IR (KBr, cm^{-1}): 3431m, 1724s, 1593w 1513w, 1431m, 1409m, 1275m, 1238s, 1187s, 1141m, 1079m, 1022m, 885w, 851m, 800w, 712m, 624m, 571m, 554w. ^1H NMR [DMSO-d$_6$, 400MHz; δ(ppm)]: 9.33–9.43 (d, 2H, $J = 5.2$ Hz, phen-H); 9.12–9.20 (d, 2H, $J = 8$ Hz, phen-H); 8.443 (s, 2H, phen-H); 8.23-8.34 (m, 2H, phen-H); 7.75–7.78 (dd, 1H, sb-H); 7.65–7.69 (dd, 1H, sb-H); 7.39–7.52 (m, 2H, sb-H). ^{13}C-NMR [DMSO-d$_6$, 400 MHz; δ(ppm)]: 167.6, 152.6, 145.9, 144.1, 141.6, 131.0, 130.8, 130.6, 129.6, 128.1, 127.0, 126.5. Calcd for $PdC_{38}H_{26}O_{10}N_4S_2$: C, 52.51%; H, 2.99%; N, 6.45%. Found: C, 52.55%; H, 2.95%; N, 6.28%.

Complex **1** can also be synthesized by hydrothermal synthesis. A mixture of palladium(II) acetate (0.015 g, 0.0668 mM), 2-sulfobenzoic acid (0.059 g, 0.267 mM), 1,10-phenanthroline (0.026 g, 0.131 mM) and H_2O (16 mL) was placed in a 30-mL stainless-steel reactor with a Teflon liner and heated at 120 °C for two days. After cooling, the resulting solution was set aside and 16 days later yellow block crystals were obtained by filtration. Yield: 83.3%.

2.2.2. Preparation of [Pd(phen)$_2$](2-Hsb)·(2-Hsb)·2H$_2$O (2). A mixture of palladium(II) acetate (0.015 g, 0.0668 mM), 2-sulfobenzoic acid (0.059 g, 0.267 mM), 1,10-phenanthroline (0.053 g, 0.267 mM), acetonitrile (5 mL) and H_2O (10 mL) was placed in a 30 mL stainless-steel reactor with a Teflon liner and heated at 120 °C for 2 days. After cooling, the resulting solution was set aside and 4 days later orange-yellow block crystals were obtained by filtration. Yield: 78.6%. IR (KBr, cm^{-1}): 3415m, 3372m, 1727s, 1701m, 1588w, 1435m, 1222m, 1183s, 1141m, 1078m, 1020s, 879w, 851m, 788w, 768w, 712s, 642w, 615s, 570w, 552m. ^{1}H NMR [DMSO-d$_6$, 400 MHz; δ(ppm)]: 9.35–9.43 (d, 2H, $J = 5.2$ Hz, phen-H); 9.17–9.25 (d, 2H, $J = 7.6$ Hz, phen-H); 8.403 (s, 2H, phen-H); 8.29–8.37 (m, 2H, phen-H); 7.78–7.81 (dd, 1H, sb-H); 7.69–7.72 (dd, 1H, sb-H); 7.41–7.55 (m, 2H, sb-H). ^{13}C-NMR [DMSO-d$_6$, 400 MHz; δ(ppm)]: 167.7, 152.6, 145.8, 144.1, 141.6, 130.9, 130.7, 130.6, 130.5, 129.6, 128.1, 126.9, 126.5. Calcd for $PdC_{38}H_{30}O_{12}N_4S_2$: C, 50.42%; H, 3.32%; N. 6.19%. Found: C, 50.31%; H, 3.21%; N, 6.22%.

2.2.3. Preparation of [Pd(phen)$_2$]·[Pd(phen)(2-sb)$_2$]·6H$_2$O (3). A mixture of palladium (II) acetate (0.015 g, 0.0668 mM), 2-sulfobenzoic acid (0.029 g, 0.134 mM), 1,10-phenanthroline (0.026 g, 0.134 mM) and H_2O (15 mL) was placed in a 30 mL stainless-steel reactor with a Teflon liner and heated at 150 °C for 24 h. After cooling, the resulting solution was set aside and 10 days later yellow needles were obtained by filtration. Yield: 60.4%. IR (KBr, cm^{-1}): 3449s, 1582s, 1560w, 1420m, 1390s, 1343w, 1233m, 1206s, 1144w, 1086w, 1022m, 840s, 775w, 736w, 710m, 661w, 622m, 570w. Calcd for $Pd_2C_{50}H_{41}N_6S_2O_{16}$: C, 47.70%; H, 3.26%; N, 6.68%. Found: C, 47.72%; H, 3.37%; N, 6.47%.

Complexes **1**, **2,** and **3** are all soluble in water, methanol, acetonitrile, DMF, and DMSO, but are insoluble in ethanol and dichloromethane.

2.3. *Crystallography*

X-ray diffraction measurements for single crystals with suitable size were performed under ambient conditions with a Bruker Smart CCD area detector equipped with graphite -monochromated Mo-Kα radiation ($\lambda = 0.71073$ Å). Data reductions were made using SAINT software [16]. An empirical absorption correction was applied by SADABS [17]. The three structures were solved by the heavy-atom method and successive Fourier syntheses. All non-H atoms were refined anisotropically against F^2 for all reflections using SHELXL-97 [18]. All hydrogens on C and carboxyl hydrogens were placed at calculated positions and refined isotropically. Hydrogens attached to water oxygens except two disordered waters in **3** were located in the difference Fourier maps and refined with isotropic displacement coefficients. WinGX and Platon software were used for the structural solution, refinement, and drawing [19, 20]. Crystallographic data and refinement parameters for **1–3** are listed in table 1.

Table 1. Crystallographic data and refinement parameters for **1–3**.

Complex	**1**	**2**	**3**
Empirical formula	$C_{38}H_{26}N_4O_{10}PdS_2$	$C_{38}H_{30}N_4O_{12}PdS_2$	$C_{50}H_{44}N_6O_{16}Pd_2S_2$
Mr	869.17	905.18	1261.83
Crystal system	Triclinic	Triclinic	Monoclinic
Space group	*P-1*	*P-1*	$P2_1/n$
Size (mm^3)	0.28 × 0.35 × 0.38	0.32 × 0.38 × 0.42	0.12 × 0.13 × 0.38
Habit/color	Yellow/block	Orange yellow/block	Yellow/needle
a (Å)	8.6706(4)	9.7664(5)	16.4934(5)
b (Å)	10.4966(6)	12.2108(6)	17.2111(5)
c (Å)	10.9538(6)	15.4209(9)	17.3664(5)
α (°)	63.263(5)	106.437(5)	90
β (°)	88.845(4)	92.526(4)	93.461(3)
γ (°)	70.973(5)	91.681(4)	90
V (Å^3)	832.19(9)	1760.48(17)	4920.8(3)
Z	1	2	4
D_{Calcd} (Mg m^{-3})	1.734	1.708	1.703
μ (mm^{-1})	0.755	0.721	0.896
θ Range	3.0–25.1	2.8–25.1	3.0–25.1
Unique reflections	2964	6269	8749
Observed reflections	2804	5309	6831
Parameters	250	526	719
$F(000)$	440	920	2552
T(K)	295(2)	295(2)	295(2)
R_1, wR_2 [$I > 2\sigma(I)$]	0.027, 0.077	0.036, 0.077	0.032, 0.069
R_1, wR_2 [all data]	0.029, 0.079	0.048, 0.085	0.051, 0.079
GOF	0.945	1.101	1.032
Largest peak and hole (e Å^{-3})	0.354, −0.399	0.404, −0.818	0.457, −0.449

2.4. *Catalytic reaction*

A 25 mL round-bottom flask was charged with a mixture of the catalyst (0.015 mM or 0.015 mM complex and 0.01 mM 2-H_2sb) in CH_3CN (5 mL) or CH_3OH (5 mL) and the substrate methyl phenyl sulfide (MPS, 0.5 mM). Then the mixture was stirred at 30 °C for 10 min. Reaction was started by addition of the corresponding amount of H_2O_2 solution (30%, 1.5 mM) under stirring. The first sample was taken after 30 min and the later samples were taken at a fixed interval of 30 min. The samples were measured by gas chromatography. The catalytic reactions were kept for 300 min.

3. Results and discussion

3.1. *Reaction chemistry*

Complex **1** can be synthesized by mixed solution method and hydrothermal synthesis. Both **2** and **3** were synthesized by hydrothermal synthesis. To explore the influencing factors in the syntheses of three complexes, we changed synthetic methods, starting materials, ratio of starting materials, reaction time, reaction temperature, and organic solvents. In CH_3CN/CH_3OH, ratios of 1 : 1 : 1, 1 : 2 : 1, 1 : 2 : 2, 1 : 4 : 2 and 1 : 4 : 4 for Pd^{II} : 2-sb : phen were investigated and only the ratios of 1 : 4 : 2 and 1 : 4 : 4 yield **1**. At the fixed molar ratio of 1 : 4 : 2 for Pd^{II}: 2-sb:phen **1** was also obtained in CH_3CN/DMF, CH_3CH_2OH/DMF and CH_3CN/H_2O.

All three complexes can be obtained by hydrothermal synthesis, while ratio of starting materials, reaction time, reaction temperature and organic solvents are different. Complex **1** was obtained when the ratio of starting materials is 1 : 4 : 2 for Pd^{II} : 2-sb : phen at 120 °C for two days in water. When the ratio of starting materials of Pd^{II} : 2-sb : phen changed to 1 : 4 : 4 at 120 °C for two days in CH_3CN/H_2O, **2** could be obtained. Complex **3** could be synthesized when the ratio of starting materials of Pd^{II} : 2-sb : phen is 1 : 2 : 2 at 150 °C for one day in water.

To ensure the phase purity of these three complexes we measured the powder X-ray diffractions and compared them with those of the single crystal diffraction simulation patterns (figures S1–S3, See http://dx.doi.org/10.1080/00958972.2013.867032 for supplemental data). The patterns of the powder X-ray diffraction for **1**, **2,** and **3** match well with the simulated ones from single crystal data. The small differences in diffraction intensities should be due to the preferred orientation of the powder samples.

3.2. *IR analysis*

Comparing IR spectra of 2-sulfobenzoic acid, the characteristic absorption peaks of –COOH at 1724 cm^{-1} in **1** and 1727 cm^{-1} in **2** are present, indicating the presence of carboxyl proton, while this peak is absent in **3**, indicating deprotonated carboxyl. In **1–3**, the band around 3440 cm^{-1} indicates the presence of ν(O–H) of lattice water. The stretching frequency of 711 cm^{-1} in **1–3** indicates the presence of phen. Peaks at 1560 and 1390 cm^{-1} are for $\nu_{as}(CO_2^{2-})$ and $\nu_s(CO_2^{2-})$ in **3**, indicating the existence of coordinated carboxyl; such peaks are absent in **1** and **2**, which corresponds with the crystal structural analysis. The characteristic vibrations of SO_3^- are at 1238, 1212 and 1187 cm^{-1} in **1**, at 1276, 1222 and 1183 cm^{-1} in **2**, and at 1233 and 1206 cm^{-1} in **3** for $\nu_{as}(SO_3^-)$, and at 1079 and 1022 cm^{-1} in **1**, 1078 and 1020 cm^{-1} in **2**, and 1086 and 1022 cm^{-1} in **3** for $\nu_s(SO_3)$.

3.3. *Crystal structures*

All three complexes consist of Pd(II), 2-sulfobenzoate, and phen but have different compositions and structures.

Complex **1** is a cation–anion species with no solvent molecule. Hsb^- are counter ions in the structure. The Pd(II) is square-planar completed by four nitrogen donors from two 1,10-phenanthroline (figure 1 and table 2). There are no intermolecular hydrogen bonds or π–π interactions in **1**. The Pd–N bond lengths vary from 2.0446(19) to 2.0468(19) Å, close to those reported in Pd(II) 1,10-phenanthroline complexes [21, 22].

Complex **2** is also an ionic species. Pd^{II} has a square pyramidal geometry completed by four N donors from two 1,10-phen and one O from sulfonate (Pd1-O4) as a very weak coordination bond with a distance of 3.107(2) Å, shorter than the sum of van der Waals radii of Pd^{II} and O^{2-} [23] (figure 2). The Pd–N bond lengths vary from 2.022(2) to 2.053 (3) Å, which are similar to those in **1**. One of two 2-Hsb^- ligands weakly coordinates to Pd^{II} ion. There are strong π–π interactions between phen rings from neighboring molecules in **2**. Hydrogen bonds between 2-Hsb^- and water and 2-Hsb^- form a 1D anionic chain (table S1).

In **3** there are two Pd ions in the asymmetric unit. Pd1 adopts six-coordinate geometry with two longer distances completed by two N donors from one phen and four O from two carboxylates (figure 3). Pd2 also affords a six-coordinate geometry with two longer distances completed by four N donors from two phen and two O from one sulfobenzoate. Considering the

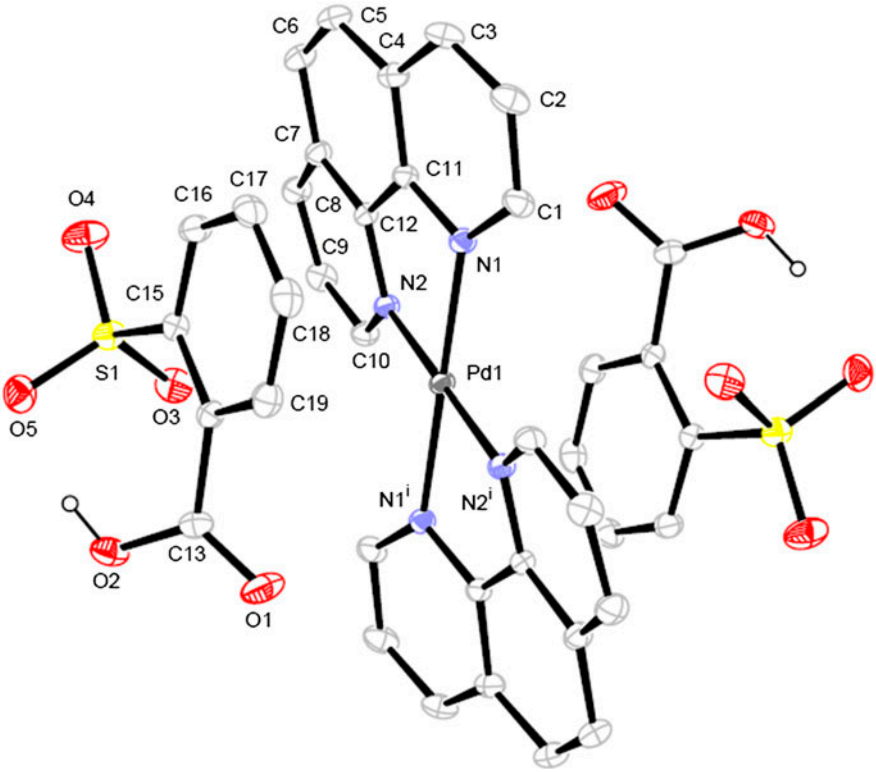

Figure 1. ORTEP view of the asymmetric unit of **1** with the labeling scheme. Hydrogens on C are omitted for clarity.

weak bonding interactions the structure of **3** is a dimer with Pd…Pd distance of 4.5694(4) Å. There are π–π interactions between phen molecules and between phen and sb^{2-}. The complex has hydrogen bonds between water molecules and between water and sb^{2-}, and these hydrogen bonds extend the structure into a 3-D hydrogen bonding architecture (table S2).

3.4. *TG analysis*

The TG curves of **1**, **2,** and **3** are shown in figure S4. Complex **1** has no solvent and is stable up to 245 °C. For **2**, from 100 to 120 °C the weight loss of 4.53% was attributed to the loss of two lattice waters (Calcd 3.98%). Complex **2** started to decompose at 247 °C. For **3**, the six lattice waters were lost from 60 to 100 °C (Calcd 8.59%, observed 8.32%). Complex **3** started to decompose at 240 °C. These three complexes have similar decomposition temperature after the removal of the lattice water molecules.

3.5. *Spectra of UV–vis*

The UV–vis absorption spectra of **1–3** and related organic ligands (2-sulfobenzoic acid and 1,10-phenanthroline) in methanol at 10^{-5} M/L at room temperature are shown in figure S5. Absorption peaks and values of molar absorption coefficient are listed in table S3.

Table 2. Selected bond lengths (Å) and angles (°) for **1–3**.

Complex **1**			
Pd1–N1	2.0446(19)	Pd1–N2	2.0468(19)
N1–Pd1–N2	80.18(7)	N1–Pd1–N2^{i}	99.82(7)
Complex **2**			
Pd1–N1	2.053(3)	Pd1–N2	2.022(2)
Pd1–N3	2.044(3)	Pd1–N4	2.036(3)
Pd1–O4	3.107(2)		
N1–Pd1–N2	80.57(10)	N1–Pd1–N3	103.1(1)
N1–Pd1–N4	163.29(10)	N2–Pd1–N3	167.59(10)
N2–Pd1–N4	99.34(10)	N3–Pd1–N4	80.58(10)
Complex **3**			
Pd1–N1	1.996(3)	Pd1–N2	2.012(3)
Pd1–O1	1.992(2)	Pd1–O2	3.173(2)
Pd1–O6	2.940(2)	Pd1–O7	2.015(2)
Pd2–N3	2.055(3)	Pd2–N4	2.031(3)
Pd2–N5	2.045(3)	Pd2–N6	2.030(3)
Pd2–O7	3.234(2)	Pd2–O9	3.275(3)
N1–Pd1–N2	82.12(11)	N1–Pd1–O1	173.54(10)
N1–Pd1–O7	93.04(10)	N2–Pd1–O1	97.44(10)
N2–Pd1–O7	175.11(10)	O1–Pd1–O7	87.45(9)
N3–Pd2–N4	80.23(11)	N3–Pd2–N5	100.96(11)
N3–Pd2–N6	178.75(11)	N4–Pd2–N5	176.33(10)
N4–Pd2–N6	98.52(11)	N5–Pd2–N6	80.29(11)

The symmetry code, i = 2−*x*, −*y*, 1−*z*.

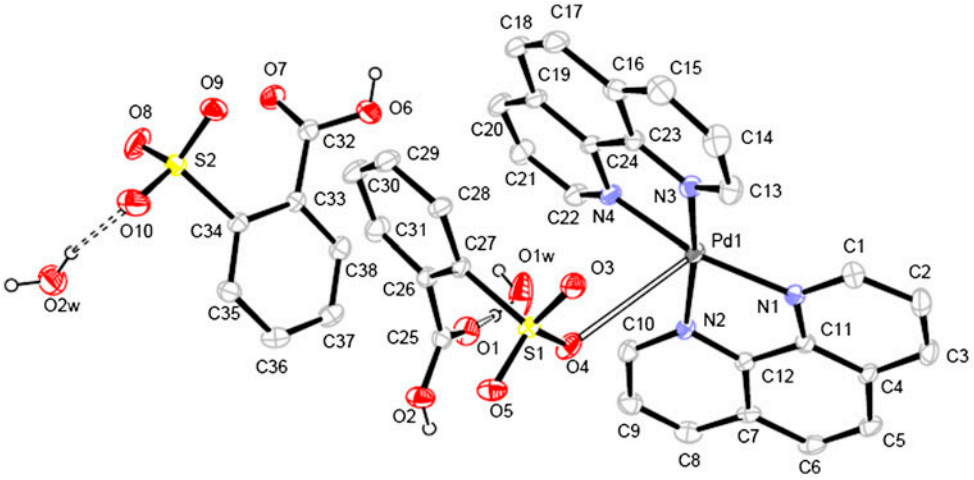

Figure 2. ORTEP view of the asymmetric unit of **2** with the numbering scheme. Hydrogen bonds are drawn as dashed lines. The open line represents weak bonding. Hydrogens on C are omitted for clarity.

Complexes **1–3** have absorption bands at 224 and 267 nm, which are attributed to π–π* transitions of phen. The former absorption is somewhat blue-shifted and the latter is slightly red-shifted compared with those of the free phen, which may be caused by the coordination of the ligand.

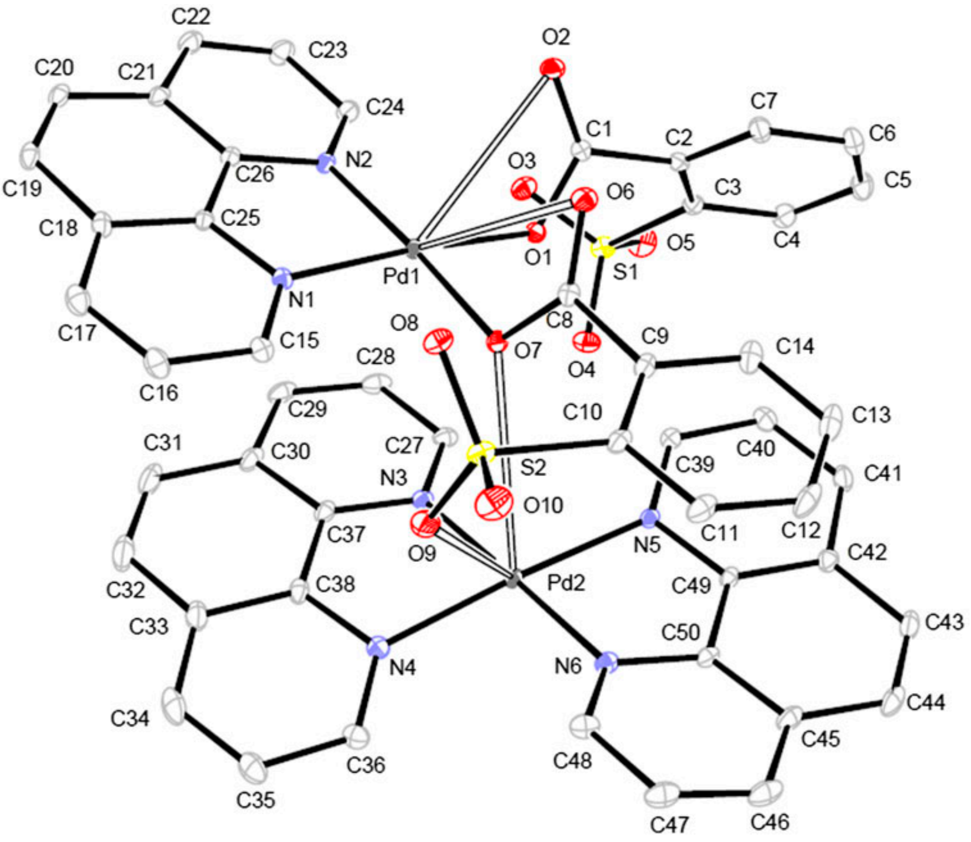

Figure 3. ORTEP view of the asymmetric unit of **3** with the numbering scheme. The open lines represent weak bonding. Hydrogens and lattice water molecules are omitted for clarity.

Table 3. The catalytic results of **1–3**.

Catalyst	Solvent	Time (min)	Conversion (%)	Selectivity (%)
Blank	CH_3CN	300	0	0
Complex **1**	CH_3CN	300	31	75
Complex **2**	CH_3CN	300	44	75
Complex **3**	CH_3CN	300	38	73
Complex **1** + 2-H_2sb	CH_3CN	300	99	87
Complex **2** + 2-H_2sb	CH_3CN	300	99	88
Complex **3** + 2-H_2sb	CH_3CN	300	99	89
Complex **1**	CH_3OH	300	93	95
Complex **2**	CH_3OH	300	94	96
Complex **3**	CH_3OH	300	99	96

Notes: Selectivities and conversions were calculated from the equations: selectivity = [sulfoxides]/[consumed sulfides] × 100; conversion = [consumed sulfides]/[initial sulfides] × 100, respectively.

3.6. *Catalytic activity*

The catalytic properties of **1–3** on oxidation of MPS (scheme 1) in acetonitrile or methanol at room temperature were investigated and the results are shown in figures 4–6 and listed in

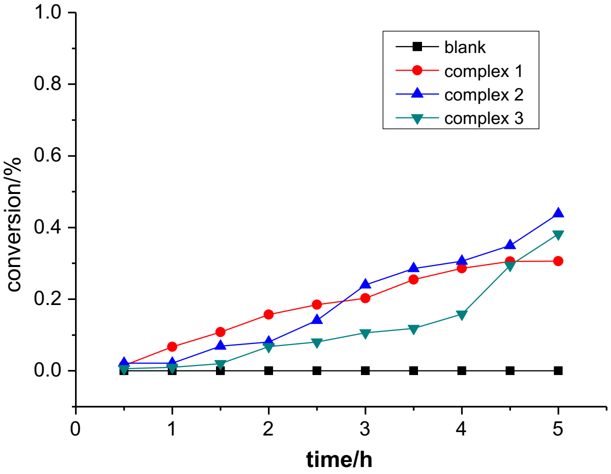

Figure 4. The conversion of MPS with the catalysts in CH_3CN.

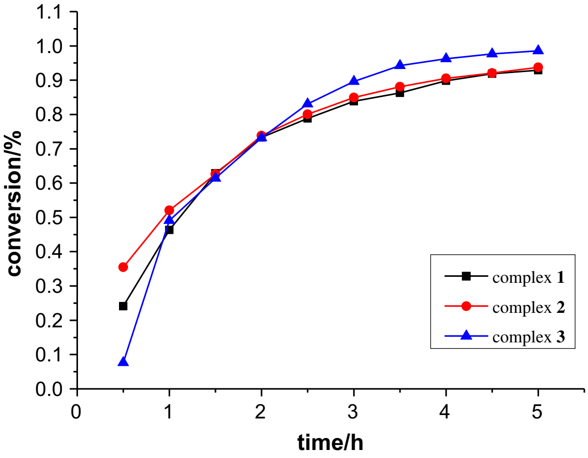

Figure 5. The conversion of MPS with the catalysts in CH_3OH.

table 3. Optimal reaction conditions are: in 6 mL of specific solvent 2 mM of MPS and 3 equiv. of H_2O_2 with a catalyst loading of 0.04 mM at $23 \pm 2\pi$ °C. A blank reaction in the absence of any catalyst under optimized reaction conditions was also performed.

Acetonitrile is frequently used in oxygenation of organic sulfides. We also checked the catalytic activity for the three Pd^{II} complexes in acetonitrile and the results are relatively poor (figure 4 and table 3), but they exhibited significantly higher activity than that of the blank experiment, indicating that these complexes have catalytic activity on oxidation of MPS. In methanol the conversion for the oxidation of MPS was significantly improved (figure 5) and the selectivity for sulfoxide is more than 95%.

It has been reported that acids affect oxidation of MPS [24]. Therefore, we added a small mount of 2-H_2sb (0.5%, 0.01 mM) in the reaction system together with the palladium

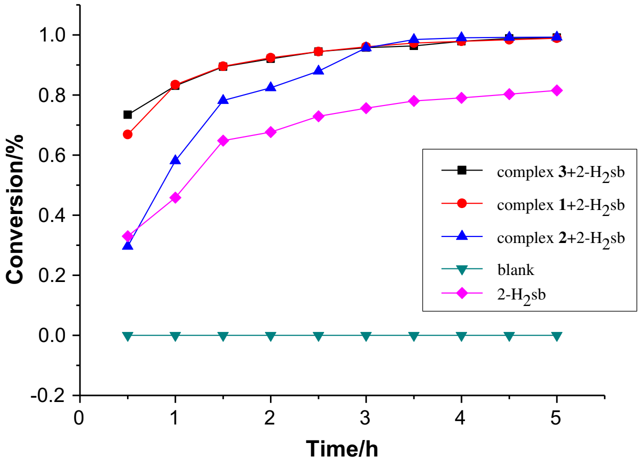

Figure 6. The conversion of MPS with the catalysts under the addition of 2-H_2sb in CH_3CN.

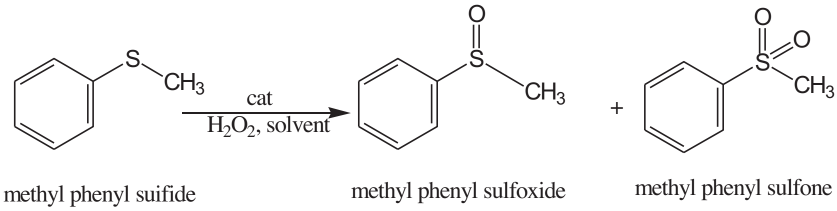

Scheme 1. The oxidation of MPS.

complexes in CH_3CN. The conversion for the oxidation of MPS is greatly improved (figure 6).

These three complexes have the same components with different structures and their catalytic activities are in the order **3** > **2** > **1**. Previous reports have supported that the bi-palladium(II) complexes have more catalytic activity, possibly due to the cooperative effect of two metals [25–27]. Our catalytic results also show that **3** is more active in the oxidation of MPS than **1** and **2**. Although the dimeric structure of **3** is formed by weak Pd–O bonds, the collective contribution of four weak bonds in **3** may provide a role in promotion of catalytic activity.

Oxygenation of MPS has attracted much attention. Bagherzadeh and his coworkers reported several investigations for such reaction using urea hydrogen peroxide as oxidant. The catalyst of Mn(III) complex with a 2-(2′-hydroxyphenyl)-5,6-dihydro-1,3-oxazine ligand in the presence of imidazole gave 71% conversion and 77% selectivity to sulfoxide [28] and Fe_3O_4@SiO_2@VO(salen) nanoparticles or VO(salen)Cl in the CH_2Cl_2/MeOH catalyzed the oxygenation reaction with >99% conversion and 95 and 100% of selectivity, respectively [29]. An oxido-peroxido tungsten(VI) complex and piperazine-bridged Mo(VI) polymer also exhibited high conversion and selectivity [30, 31]. Jin also did oxygenation of MPS using hydrogen peroxide as oxidant catalyzed by dioxomolybdenum(VI) complex and the results showed that the conversion is 80% within one hour [32]. Compared with these non-palladium catalysts, our palladium complexes (especially **3**) exhibit high catalytic activity.

4. Conclusion

Three palladium complexes with the same components were synthesized and characterized. Desolvated complexes have similar decomposition temperatures. Complexes **1–3** have some differences in the absorption strength and peak positions of the electric spectra. The catalytic oxidation of MPS in methanol at ambient temperature using **1–3** as homogenous catalysts gave excellent efficiency and is significantly higher than those in acetonitrile. The dimeric complex **3** showed the highest catalytic activity. Moreover, the acid of 2-H_2sb can promote the conversion, indicating that these palladium complexes are potential candidates for oxidation of organic sulfides.

Supplementary material

Hydrogen bonding parameters of **1** and **2** (tables S1 and S2); powder X-ray analysis for **1**–**3** (figures S1–S3); TG curves of **1–3** (figure S4); UV–vis spectra and data (figure S5 and table S3); crystallographic data in CIF format (CCDC of CCDC 959888–959890).

Funding

This work is supported by the National Natural Science Foundation of China [grant number 21073157].

References

[1] (a) C.S. Liu, J.R. Li, C.Y. Li, J.J. Wang, X.H. Bu. *Inorg. Chim. Acta*, **360**, 2532 (2007); (b) H. Pruchnik, T. Lis, M. Latocha, A. Zielinska, S. Ulaszewski, I. Pelinska, F.P. Pruchnik. *J. Inorg. Biochem.*, **111**, 25 (2012).

[2] (a) T. Kurc, J. Janczak, J. Hoffmann, V. Videnova-Adrabinska. *Cryst. Growth Des.*, **12**, 2613 (2012); (b) J. Zhang, L.G. Zhu. *Acta Crystallogr.*, **C63**, o484 (2007).

[3] (a) P. Thuery. *Inorg. Chem.*, **52**, 435 (2013); (b) P. Thuery. *Cryst. Growth Des.*, **12**, 1632 (2012); (c) P. Thuery. *Cryst. Growth Des.*, **11**, 5702 (2011).

[4] (a) X.F. Zheng, L.G. Zhu. *J. Mol. Struct.*, **1039**, 1 (2013); (b) X.F. Zheng, L.G. Zhu. *Polyhedron*, **30**, 666 (2011); (c) X.F. Zheng, L.G. Zhu. *Inorg. Chim. Acta*, **365**, 419 (2011); (d) X.F. Zheng, L.G. Zhu. *CrystEng-Comm*, **12**, 2878 (2010); (e) X.H. Miao, L.G. Zhu. *New J. Chem.*, **34**, 2403 (2010).

[5] (a) H.C. Garcia, R. Diniz, L.F.C. De Oliveira. *Polyhedron*, **53**, 40 (2013); (b) S. Song, X. Li Y.H. Zhang. *Dalton Trans.*, **42**, 10409 (2013); (c) Q.Y. Liu, Z.J. Xiahou, Y.L. Wang, L.Q. Li, L.L. Chen, Y. Fu. *CrystEng-Comm*, **15**, 4930 (2013).

[6] (a) X.F. Li, Y.B. Huang, R. Cao. *Dalton Trans.*, **41**, 6195 (2012); (b) X.F. Zheng, L.G. Zhu. *Cryst. Growth Des.*, **9**, 4407 (2009).

[7] L.M. Mirica, J.R. Khusnutdinova. *Coord. Chem. Rev.*, **257**, 299 (2013).

[8] (a) J. Granell, M. Martinez. *Dalton Trans.*, **41**, 11243 (2012); (b) S. Hohloch, W. Frey, C.Y. Su, B. Sarkar. *Dalton Trans.*, **42**, 11355 (2013); (c) D.Y. Ma, L.X. Zhang, X.Y. Rao, T.L. Wu, D.H. Li, X.Q. Xie. *J. Coord. Chem.*, **66**, 1486 (2013).

[9] (a) S. Akkoc, Y. Gok. *J. Coord. Chem.*, **66**, 1396 (2013); (b) A. Kumar, G.K. Rao, A.K. Singh. *RSC Advances*, **2**, 12552 (2012).

[10] S. Mecking. *Coord. Chem. Rev.*, **203**, 325 (2000).

[11] A. Garoufis, S.K. Hadjikakou, N. Hadjiliadis. *Coord. Chem. Rev.*, **253**, 1384 (2009).

[12] F.H. Allen. *Acta Crystallogr.*, **B58**, 380 (2002).

[13] G.J. Grant. *Dalton Trans.*, **41**, 8745 (2012).

[14] (a) J.C. Hierso, R. Feurer, P. Kalck. *Coord. Chem. Rev.*, **178**–**180**, 1811 (1998); (b) J. Vicente, A. Arcas. *Coord. Chem. Rev.*, **249**, 1135 (2005); (c) V.K. Jain, L. Jain. *Coord. Chem. Rev.*, **254**, 2848 (2010); (d) O. Yamauchi, T. Yajima, R.Fujii, Y. Shimazaki, M. Yabusaki, M. Takani, M. Tashiro, T. Motoyama, M. Kakuto, Y. Nakabayashi. *J. Inorg. Biochem.*, **102**, 1218 (2008).

[15] A. Bacchi, M. Carcelli, P. Pelagatti. *Crystallogr. Rev.*, **18**, 253 (2012).

[16] SMART and SAINT. *Area Detector Software Package and SAX Area Detector Integration Program*, Bruker Analytical X-ray, Madison, WI (1997).

[17] G.M. Sheldrick. *SADABS, Program for Bruker Area Detector Absorption Correction*, University of Göttingen, Germany (1997).

[18] G.M. Sheldrick. *SHELXL-97, Program for Crystal Structure Refinement*, University of Göttingen, Germany (1997).

[19] L.J. Farrugia. *J. Appl. Crystallogr.*, **32**, 837 (1999).

[20] A.L. Spek. *Acta Crystallogr.*, **D65**, 148 (2009).

[21] (a) E. Guney, V.T. Yilmaz, O. Buyukgungor. *Inorg. Chim. Acta*, **363**, 2416 (2010); (b) E. Guney, V.T. Yilmaz, C. Kazak. *Polyhedron*, **29**, 1285 (2010).

[22] (a) V.T. Kasumov, E. Sahin. *Spectrochim. Acta, Part A*, **107**, 31 (2013); (b) J.R. Pioquinto-Mendoza, D.G. Olvera-Mendoza, N. Andrade-Lopez, J.G. Alvarado-Rodriguez, R. Moreno-Esparza, M. Flores-Alamo. *J. Coord. Chem.*, **66**, 2477 (2013).

[23] A. Bondi. *J. Phys. Chem.*, **68**, 441 (1964).

[24] W.T. Hu, L.G. Zhu. *Chin. J. Inorg. Chem.*, **29**, 1109 (2013).

[25] A. Zanardi, J.A. Mata, E. Peris. *Organometallics*, **28**, 4335 (2009).

[26] S.K. Yen, L.L. Koh, H.V. Huynh, T.S.A. Hor. *Chem. Asian J.*, **3**, 1649 (2008).

[27] N.D. Jones, B.R. James. *Adv. Synth. Catal.*, **344**, 1126 (2002).

[28] M. Amini, M. Bagherzadeh, Z. Moradi-Shoeili, D.M. Boghaei, A. Ellern, L.K. Woo. *J. Coord. Chem.*, **66**, 464 (2013).

[29] M. Bagherzadeh, M.M. Haghdoost, A. Shahbazirad. *J. Coord. Chem.*, **65**, 591 (2012).

[30] M. Amini, M. Bagherzadeh, B. Eftekhari-Sis, A. Ellern, L.K. Woo. *J. Coord. Chem.*, **66**, 1897 (2013).

[31] M. Bagherzadeh, M. Zare. *J. Coord. Chem.*, **66**, 2885 (2013).

[32] N.Y. Jin. *J. Coord. Chem.*, **65**, 4013 (2012).